Check for updates

OPEN

Low geomagnetic field strength during End-Cretaceous Deccan volcanism and whole mantle convection

Radhakrishna T.[1,3] ✉, Asanulla R. Mohamed[1], Venkateshwarlu M.[2] & Soumya G. S.[1,4]

Knowledge about long-term variation of the geomagnetic dipole field remains in its nascent stage because of the paucity of reliable experimental data over geological periods. Here, we present the first robust experimental data from the largest Cretaceous flood basalt province on Earth, the ~65–66 Ma Deccan basalt within a thick (1250 m) unbiased stratigraphic section down to the basement, recovered from a drill hole of the Koyna Deep Scientific Drilling Project in the Western Ghats, India. Critical analysis of the result along with similar results of the Cretaceous age find that (i) the dipole moment during the end Cretaceous Deccan eruption is the lowest in whole of Cretaceous (ii) dipole moment at the onset/termination of the Cretaceous Normal Superchron is apparently lower relative to that in mid-superchron, however, such differences cannot be deciphered in shorter polarities probably because of insufficient time to develop recognizable variations (iii) inverse relation between dipole moment and reversal rate is lacking and (iv) a cause and effect relation between core-mantle boundary heat flux and low dipole moment that appears to be the principle governing factor in forming the Large Igneous Provinces on the surface of earth.

Long-term variability of Earth's early Dipole magnetic field (palaeointensity; PI) is a complex internally driven phenomenon. Numerical simulations apart, geological materials are the only source for direct experimental estimates. However, large failure rate, prolonged duration of experiments and increased complexities in deciphering magnetic field at early periods have become a serious hindrance for this experimental approach; therefore, a vast number of studies have focused over the period of one million year, where the determinations are relatively more straight forward. Yet, in recent years, there have been compilations of PI data over the geological period with an objective to develop a robust global database (for example, PINT15 database: http:// earth.liv.ac.uk /pint/).

The Mesozoic period has drawn a special attention with the proposal of a period of relatively low field, one-third of the Cenozoic value, known as the Mesozoic Dipole Low (MDL)[1]. Whereas some investigations argue that the MDL proposal is not tenable[2–6], the hypothesis has gained wider support[7–9] although many disagreements exist on the duration of the low field. The MDL was suggested to confine to the Jurassic Quiet Zone (~145–165 Ma)[10], and some others extend it into early Cretaceous[11–13]. The low field strength is also variably described with respect to the Cretaceous Normal Superchron (CNS); some argue that the MDL extended into the CNS[14,15], some others, mostly from China, report a low field at the onset of CNS[16–18] and some works find it at the end of the CNS[19–22]. Likewise, the low fields are correlated with high reversal frequency[9,23–26], but there are arguments decoupling the two[21,27,28]. The fluctuation in geomagnetic field strength is intricately linked to core-mantle boundary (CMB) heat flow and whole mantle convection processes[25,29–32]. In light of the ongoing hot debate and the large-scale geodynamic significance, we conducted a comprehensive PI study on one of the prominent surface manifestations of whole mantle convection, the Deccan flood basalt covering an unbiased stratigraphic section within a thick drill hole of the Continental Scientific Deep Drilling Project in the Koyna region of the Western Ghats, India (Fig. 1). We combine the results with other high quality Cretaceous global data and interpret in terms of relationships between geomagnetic behavior, polarity reversals and deep mantle processes.

[1]National Centre for Earth Science Studies, Trivandrum, 695011, India. [2]CSIR-National Geophysical Research Institute, Hyderabad, 500 007, India. [3]Present address: GITAM University, Nagadenehalli, Doddaballapur Taluk, Bengaluru, 561203, India. [4]Present address: Department of PG Studies and Research in Geology, Government College Kasaragod, Vidyanagar, 671123, India. ✉e-mail: tradha1@rediffmail.com
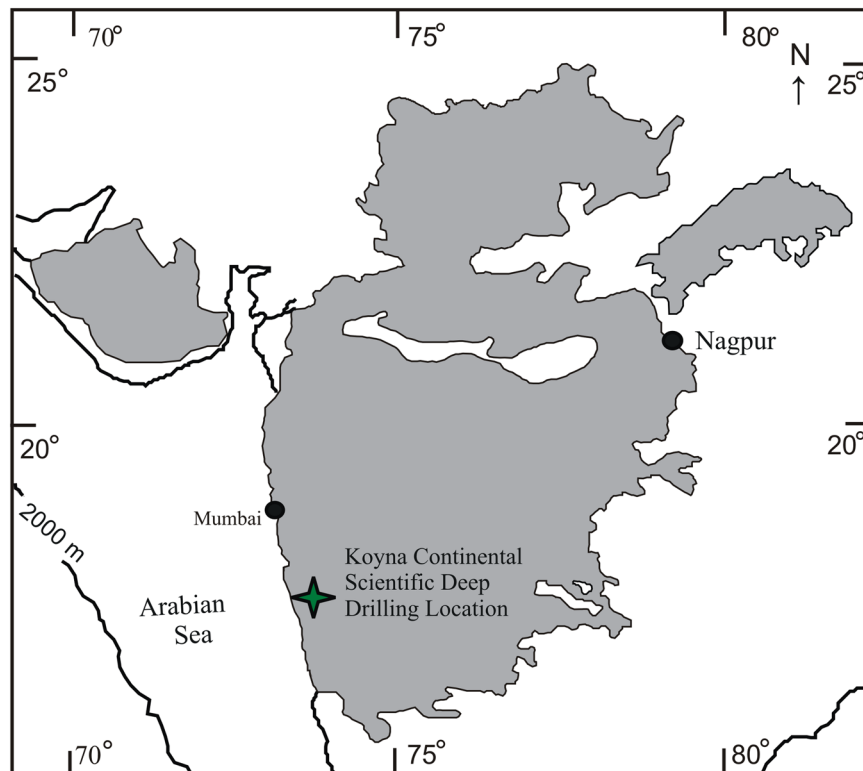
Figure 1. Geological map showing areal spread of the Deccan flood basalt eruptions and location of the Koyna Continental Scientific Deep Drilling Project drill hole (KBH-7) of this study.

Materials and Methods

The Koyna Deccan basalt drill hole (KBH-7) samples of the present PI study come from nineteen flows comprising of 1250 m thick lava sequence down to the Archaean gneissic basement. The lava pile represents the stratigraphic formations that constitute the Wai Group. The top ~350 m section belongs to the Mahabaleswar formation with normal polarity and thereafter, the section down to the basement is monotonously of reverse polarity that represents the Ambenali, upper Poladpur and lower Poladpur formations in succession downwards[33]. The drill hole section recovered at least seven red boles amounting to a thickness of more than 5 m and a few alteration zones indicating that smaller pulses of eruptions are separated by longer times of volcanic quiescence. The time needed to form the red bole estimated a few kilo years of quiescence[34]. This suggests that several kilo years to millennia are recorded in our PI data. Recent high precision U-Pb and $^{40}Ar/^{39}Ar$ ages are an added advantage for the present study; these results unequivocally place the age of the Koyna Deccan drill hole succession at ~65–66 Ma[35,36].

PI experimental techniques and the reliability criteria have been revolutionized with pronounced modifications over the years, although the Thellier–Thellier[37] method remains more fundamental for most of the investigations. Many of the earlier results have some limitations and highlight the need for additional accurate data[28]. The PI study of the well-dated Deccan section adopted a systematic approach: determined detailed rockmagnetic properties as a prelude to PI experiments, used a more accepted thermal PI method (Zero field-In field)[38], conducted partial thermoremanent magnetization (pTRM) checks and pTRM tail checks, assessed for cooling rate and anisotropy corrections and followed standard set of strict reliability and quality criteria to consider results to compute field strength at the time (c. 65–66 Ma) of the Deccan flood basalt eruption (see details of methods in electronic supplement).

Results

Although the investigations were performed on 76 samples covering the 19 flows down to the basement, only 34 samples from nine flows were found successful in yielding PI data. A judicious selection, considering that (i) at least there are successful determinations from three independent samples (ii) the samples show within flow consistency that is within limits of standard deviation (iii) the uncertainties over the mean value of the flow are less than 20% and (iv) none of the flows represent transition field, eight lava flows (26 samples) provide a reliable mean palaeointensity of $7.30 \pm 3.45 \mu T$. Using the remarkably well constrained Deccan palaeopole (37.8°N, 282.6°E)[34], ~65 Ma palaeolatitude for the Koyna drill hole is estimated as 28.1°S to calculate the Virtual Dipole Moment (VDM),which is independent of the latitude. The calculated mean VDM is $1.46 \pm 0.69 \times 10^{22}$ Am^2 (range: 2.19–0.28 $\times 10^{22}$ Am^2; see Supplementary Table S1). Comparable values were estimated on surface samples of the Deccan (unpublished) in an independent study funded by the Indo-French Collaboration for Promotion of Advanced Research (IFCPAR). Because (a) the magnetization directions from cooling units of the formations
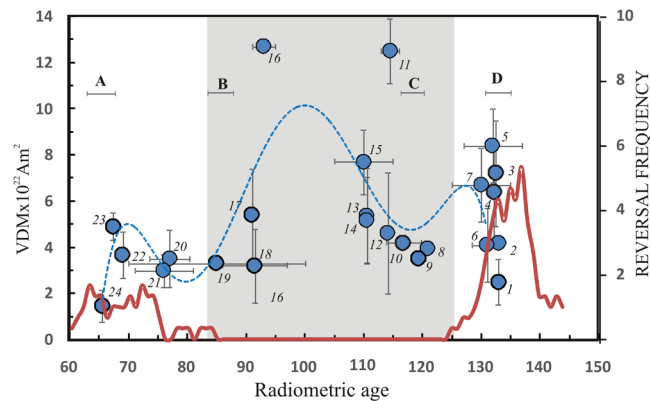
Figure 2. Distribution of VDM data during the Cretaceous period. The data set is as listed in table S-T2. Note a polynomial trend showing high dipole moment with low values on either end of the CNS. The numbers next to the data points are linked to the serial numbers in table S-T2. Also shown are the timing of mantle plumes of the Cretaceous responsible for the major large igneous provinces marked as A, B, C and D: A denotes the Reunion related Deccan flood basalt (and near synchronous ~62 Ma North Atlantic Tertiary Volcanic Province), B denotes the Marion plume related Madagascan igneous province (and near synchronous ~ 90 Ma Ontong Java plateau), C denotes the Kerguelen plume related Rajmahal volcanism and D denotes the Tristan da Cunha plume related Parana basalts. The ages of these LIPs are shown with error bars. It can be seen the low dipole moments correspond to the mantle plumes/LIPs in age. Area coverage of LIPs in each age bracket (A: >3; B: <3.5; C: ~2 and D: ~1.5 in million km^2)[49,50] may indicate a measure of their magnitudes. Polarity reversal frequency with 3 Ma running average from the 2012 GPTS[51] is shown in red line. The grey shade demarcates the CNS.

sampled in this study show that secular variation has been averaged[39] and (b) geologically an interval of kilo years to million years long has been sampled, the mean paleointensity is accepted to represent a paleomagnetic dipole moment, rather than a snapshot dipole moment. Thus, this result is the best dipole moment result from one of the two largest Phanerozoic flood basalt provinces of the world and the largest Cretaceous igneous province.

Discussion

Mesozoic dipole moments have been reported from volcanic rocks and deep sea sediments. Now, it is well known that sediment record is smoothed over time and provides relative intensity record and thus provides a continuous evolution of palaeofield strength rather than absolute PI values[40]. Furthermore, current methods to estimate absolute PI are applicable only to materials that acquired a thermal remanent magnetization by cooling in the Earth's magnetic field and volcanic rocks are the best choice to provide absolute estimates on millions and perhaps billions of years scale[41]. Not all volcanic rocks of PI investigation are constrained for their ages by radiometric methods. Also, some of the PI determinations come from submarine basaltic glass in which the magnetic minerals are sometimes chemically altered during PI experiments, and thus highlight the need to obtain the data from magnetically stable volcanic rocks to clarify the nature of geomagnetic field in the Late Cretaceous[21,28]. Furthermore, most submarine basalt glass values represent averages of data from individual samples and not the averages of independent time units constrained by lava flow stratigraphy and paleomagnetic directional analysis[23,28]. In these respects, the Koyna drill hole samples of the Deccan are a valuable resource material because these are fresh subaerial eruptions with high precision age constraints and comprise several cooling units in an unbiased stratigraphic section down to the basement. Based on all these factors, we consider here the Deccan results in combination with other Cretaceous PI results from radiometrically dated igneous rocks and obtained by the Thellier method with pTRM checks, excluding submarine basalt glass data.

The data meeting the above criteria are listed in Supplementary Table S2 and are illustrated in Fig. 2. Most striking is that the mean VDM value of the Deccan is the lowest among whole of the Cretaceous data. The combined VDM results of the Cretaceous are fitted by a polynomial trend in Fig. 2. We forced the polynomial fit to pass through our data point 24 because of its robust estimation. The trend reflects high field strength in the mid-CNS and relatively low fields on either end of the CNS. Although data are sparse for the mid-CNS period, the stronger dipole in the mid-CNS is supported by numerical models predictions[31,32]. The low VDM values during the onset and termination of the superchron are interpreted here to suggest that the polarity transitions are marked by relatively lower dipole field strength. That is, the geodynamo becomes more turbulent resulting in low VDM values while approaching a reversing regime and attains gradually a non-reversing state with high VDMs in the mid-CNS interval. Differences in the VDM fluctuations across polarity intervals of shorter time span could be so low that cannot be resolved by the present PI experimental protocols, however, should be detected on superchron scales. Studies with respect to the Permian Kiaman Long Reversed Superchron (~265–310 Ma) and the Moyero Reversed Superchron (~460–490 Ma) will be more promising to test the idea proposed here; however, reliable PI results are not available for these time frames. This study underlines the urgent need of PI investigations for these two superchron time frames.

The dipole moment variations have been linked to reversals frequency based on observed low dipole moments during the high reversal frequency middle Jurassic period (~145–65 Ma) and high dipole moments during the CNS[9,23,25,26,29,42]. The high field strength during mid-CNS and low values while entering into and coming out of CNS may be viewed as an indication for inverse relation between field strength and reversal frequency. If there is such an inverse relationship between reversal rate and dipole moment, then the dipole moment at the time of the Deccan eruption should be higher than that during the early Cretaceous (~130–135 Ma) when the reversal rate is more than double to that of the Deccan times (Fig. 2) and also it should be higher than that during mid-Jurassic and in the late Cenozoic when the reversal rates are high ($>$10 and 5 per Ma respectively). In sharp contrast, the VDM value determined for the Deccan eruption is lower than that of ~130–135 Ma (Fig. 2) and much lower than that in mid-Jurassic (for ex., a VDM of $3.27 \pm 0.49 \times 10^{22} Am^2$ at 166 Ma[9]) and the late Cenozoic (for ex., $\sim 5 \times 10^{22} Am^2$ in Miocene[43]); thus the comparison does not support inverse relation between reversal frequency and dipole moment at all times despite the coincidence of low dipole moments and high reversal frequency during mid-Jurassic[10,25,44] and Devonian[45,46].

Numerical dynamo models[25,26,29,31,32,42,47] predict a relationship between high CMB heat flux, via large-scale mantle convection, low dipole moments and high reversal frequency. We find that coupling between dipole moments and CMB heat flux appears to be evident. The low dipole moment is coincident with increased heat flow generated by hyperactive core-mantle process. In consequence, mantle plume departs from the CMB resulting in significant crustal growth at the surface by addition of huge volumes of mantle inputs that manifest in the form of large igneous provinces. The best examples are the Reunion and Marion plume inputs corresponding to the low dipole moments at the end of (and also following) the CNS; similarly the Tristan da Cunha and Kerguelen plume inputs correspond to the low fields at the onset of CNS. However, the high VDM value of the Kerguelen plume related Rajmahal traps (Supplementary Table S2 and Fig. 2) might indicate some time lag between the plume initiation at the CMB and its surface eruption[32]. The mid-Jurassic low dipole moment can be ascribed to high CMB heat flow and crustal growth linked to the Conrad mantle plume activity represented by the Karro igneous province comprising high reversal frequency (at least seven polarity transitions within one Ma)[48]. Deccan flood basalt is the largest igneous outpouring in the whole of Cretaceous and correspondingly the CMB was more hyperactive and resulted in the lowest dipole moment in the entire Cretaceous. Conversely, the mid superchron period (~95–115 Ma) is a period of near quiescence for CMB heat flow and thus mantle plume activity was lowest and high dipole moment developed. Thus our results support the coupling between the dipole moment and CMB heat flow proposed by the numerical models, but suggest that the links with reversal frequency still remain elusive and probably another ingredient also controlling reversal frequency.

Conclusion

This paper presents the first robust palaeointensity experimental data from the successive Deccan basalt lava flows of end Cretaceous age (~66–65 Ma) within a continuous drill core section of the Continental Scientific Deep Drilling Project in the Western Ghats, India. Eight lava flows provide a reliable mean VDM value ($1.46 \pm 0.69 \times 10^{22} Am^2$). The dipole moment is clearly time-averaged because the mean value is estimated using data from undisputed multiple cooling units of the fresh subaerial lava flows in an unbiased thick stratigraphic section down to the basement, covering kilo years to more than a million year time frame. The results highlight (a) Dipole moment during the end Cretaceous Deccan eruption is the lowest in the whole of Cretaceous while dipole moment is generally lower at onset/termination of Cretaceous Normal Superchron relative to mid-superchron times (b) lack of perfect inverse relation between dipole moment and field reversal rate in contrast to many studies invoking coupling between the two and (c) a cause and effect relationship between CMB heat flux and the dipole low, supporting the predictions of the numerical models; large igneous provinces are shown as manifestations of this activity on the surface of earth.

Data availability

All data generated or analyzed during this study are included in this published article (and its Supplementary Information files).

References

1. Prevot, M., Derder, M. M., McWilliams, M. & Thompson, J. Intensity of the Earth's magnetic field: Evidence for a Mesozoic dipole low. *Earth Planet. Sci. Lett.* **97**, 129–139 (1990).
2. Juarez, M. T., Tauxe, L., Gee, J. S. & Pick, T. The intensity of the Earth's magnetic field over the past 160 million years. *Nature.* **394**, 878–881 (1998).
3. Goguitchaichvili, A., Alva-Valdivia, L.M., Urrutia-Fucugauchi, J., Morales, J. & Ferreira-Lopes, O. On the Reliability of Mesozoic Dipole Low: New Absolute Paleointensity Results from Parana Flood Basalts (Brazil). *Geophys. Res. Lett.* **29(13)**, 1655, https://doi.org/10.1029/2002GL015242 (2002b).
4. Goguitchaichvili, A. *et al.* New absolute paleointensity results from the Parana Magmatic Province (Uruguay) and the Early Cretaceous geomagnetic paleofield. *Geochem. Geophys. Geosyst.* **9**, Q11008, https://doi.org/10.1029/2008GC002102 (2008).
5. Ruiz, C. R. *et al.* Early cretaceous absolute geomagnetic paleointensities from Cordoba Province (Argentina). *Earth Planets Space.* **58**(10), 1333–1339 (2006).
6. Mena, M., Goguitchaichvili, A., Solano, M. C. & Vilas, J. F. Paleosecular variation and absolute geomagnetic paleointensity records retrieved from the Early Cretaceous Posadas Formation (Misiones, Argentina). *Stud. Geophys. Geod.* **55**(2), 279–309 (2011).
7. Pick, T. & Tauxe, L. Geomagnetic palaeointensities during the Cretaceous normal superchron measured using submarine basaltic glass. *Nature.* **366**(6452), 238–242 (1993).
8. Carvallo, C., Camps, P., Ooga, M., Fanjat, G. & Sager, W. W. Palaeointensity determinations and rock magnetic properties on basalts from Shatsky Rise: new evidence for a Mesozoic dipole low. *Geophys. J. Int.* **192**, 986–999 (2013).

9. Sprain, C. J., Feinberg, T. J. M., Geissman, J. W., Strauss, B. & Brown, M. C. Paleointensity during periods of rapid reversal: A case study from the Middle Jurassic Shamrock batholith, western Nevada. *GSA Bulletin.* **128**(no. 1/2), 223–238, https://doi.org/10.1130/B31283.1;10 (2016).

10. McElhinny, M. W. & Larson, R. L. Jurassic dipole low defined from land and sea data. *Eos Trans. Am. Geophys. Union.* **84**, 362–366 (2003).

11. Kosterov, A. A. & Pr´evot, M. Possible mechanisms causing failure of Thellier palaeointensity experiments in some basalts. *Geophys. J. Int.* **134**, 554–572 (1998).

12. Tauxe, L., Gee, J. S., Steiner, M. & Staudigel, H. Paleointensity results from the Jurassic: new constraints from submarine basaltic glasses of ODP Site 801C. *Geochem. Geophys. Geosyst.* **14**, 4718–4733, https://doi.org/10.1002/2013GC004704 (2013).

13. Dodd, S. C., Muxworthy, A. R. & Niocaill, C. M. Paleointensity determinations from the Etendeka province, Namibia, support a low magnetic field strength leading up to the Cretaceous normal superchron. *Geochem. Geophys. Geosyst.* **16**, 785–797, https://doi.org/10.1002/2014GC005707 (2015).

14. Shi, R., Hill, M., Zhu, R., He, H. & Shaw, J. ^{40}Ar/^{39}Ar dating and preliminary paleointensity determination on a single lava flow from Chifeng, Inner Mongolia. *Phys. Earth Planet. Inter.* **152**, 78–89 (2005).

15. Granot, R., Tauxe, L., Gee, J. S. & Ron, H. A view into the Cretaceous geomagnetic field from analysis of gabbros and submarine glasses. *Earth Planet. Sci. Lett.* **256**, 1–11 (2007).

16. Zhu, R. *et al.* Palaeointensities determined from the middle Cretaceous basalt in Liaoning Province, northeastern China. *Phys. Earth Planet. Inter.* **142**(1), 49–59 (2004).

17. Ruiz, C. R *et al.* Absolute Thellier paleointensities from Ponta Grossa dikes (southern Brazil) and the early Cretaceous geomagnetic field strength. Geofís. Int. **48(2)** (2009).

18. Qin, H., He, H., Liu, Q. & Cai, S. Palaeointensity just at the onset of the Cretaceous normal superchron. *Phys. Earth Planet. Inter.* **187**, 199–211 (2011).

19. Zhao, X. *et al.* New palaeointensity results from Cretaceous basalt of inner Mongolia, China. *Phys. Earth Planet. Inter.* **141**, 131–140 (2004).

20. Shcherbakova, V. V., Asanidze, B. Z., Shcherbakov, V. P. & Zhidkov, G. V. Geomagnetic field paleointensity in the Cretaceous from Upper Cretaceous rocks of Georgia. *Izv. Phys. Solid Earth.* **43**(11), 951–959 (2007).

21. Chang, B., Kim, W., Doh, S. J. & Yu, Y. Paleointensity determination of Late Cretaceous basalts in northwest South Korea: implications for low and stable paleofield strength in the Late Cretaceous. *Earth Planets Space.* **65**, 1501–1513 (2013).

22. Kim, W., Doh, S. J. & Yu., Y. Reliable paleointensity determinations from Late Cretaceous volcanic rocks in Korea with constraint of thermochemical alteration. *Phys. Earth Planet. Inter.* **279**, 47–56 (2018).

23. Tarduno, J. A., Cottrell, R. D. & Smirnov, A. V. High Geomagnetic Intensity during the mid-Cretaceous from Thellier analyses of single palgioclase crystals. *Science* **291**(5509), 1779–1783 (2001).

24. Tarduno, J. A., Cottrell, R. D. & Smirnov, A. V. The Cretaceous superchron geodynamo: observations near the tangent cylinder. *Proceedings of the National Academy of Sciences.* **99**(22), 14020–14025 (2002).

25. Tarduno, J.A., & Cottrell, R.D. Dipole strength and variation of the time-averaged reversing and non-reversing geodynamo based on Thellier analyses of single plagioclase crystals. J. Geophys. Res. **110**, B11101, 10.1029JB003970 (2005).

26. Shcherbakova, V. V., Bakhmutov, V. G., Shcherbakov, V. P., Zhidkov, G. V. & Shpyra, V. V. Palaeointensity and palaeomagnetic study of Cretaceous and Palaeocene rocks from Western Antarctica. *Geophys. J. Int.* **189**, 204–228 (2012).

27. Goguitchaichvili, A., Alva-Valdivia, L. M., Rosas-Elguera, J., Urrutia-Fucugauchi, J. & Sole, J. Absolute Geomagnetic paleointensity after the Cretaceous Normal Superchron and just prior to the Cretaceous-Tertiary transition. *J. Geophys. Res.* **109**, B01105, https://doi.org/10.1029/2003JB002477 (2004).

28. Ingham, E., Heslop, D., Roberts, A. P., Hawkins, R. & Sambridge, M. Is there a link between geomagnetic reversal frequency and paleointensity? A Bayesian approach. *J. Geophys. Res. (Solid Earth)* **119**, 5290–5304, https://doi.org/10.1002/2014JB010947 (2014).

29. Larson, R. L. & Olson, P. Mantle plumes control magnetic reversal frequency. *Earth Planet. Sci. Lett.* **107**(3), 437–447 (1991).

30. Biggin, A. J. *et al.* Possible links between long-term geomagnetic variations and whole- mantle convection processes. *Nat. Geosci.* **5**, 526–533, https://doi.org/10.1038/ngeo1521 (2012).

31. Olson, P. L., Coe, R. S., Driscoll, P. E., Glatzmaier, G. A. & Roberts, P. H. Geodynamo reversal frequency and heterogeneous core-mantle boundary heat flow. *Phys. Earth Planet. Inter.* **180**, 66–79 (2010).

32. Olson, P. & Amit, H. Mantle superplumes induce geomagnetic superchrons. *Front. Earth Sci.* **3**, 38, https://doi.org/10.3389/feart.2015.00038 (2015).

33. Radhakrishna, T., Asanulla, R. M., Venkateshwarlu, M., Soumya, G. S. & Prachiti, P. K. Mechanism of rift flank uplift and escarpment formation evidenced by Western Ghats, India. *Scientific Reports-(Nature).* **9**(1), 10511, https://doi.org/10.1038/s41598-019-46564-3 (2019).

34. Chenet, A. L. *et al.* Determination of rapid Deccan eruptions across the Cretaceous–Tertiary boundary using paleomagnetic secular variation: 2. Constraints from analysis of eight new sections and synthesis for a 3500-m-thick composite section. *J. Geophys. Res.* **114**, 38, https://doi.org/10.1029/2008JB005644 (2009).

35. Schoene, B. *et al.* U-Pb constraints on pulsed eruption of the Deccan Traps across the end-Cretaceous mass extinction. *Science.* **363**, 862–866 (2019).

36. Sprain, J. C. *et al.* T. The eruptive tempo of Deccan volcanism in relation to the Cretaceous-Paleogene boundary. *Science.* **363**, 866–870 (2019).

37. Thellier, E. & Thellier., O. SUR l'intensite du champ magnetiqueterrestredans le passé historiqueetgeologique. *Ann Géophys.* **15**, 285–376 (1959).

38. Coe, R. S. Paleointensities of the Earth's magnetic field determined from Tertiary and Quaternary rocks. *J Geophys. Res.* **72**(12), 3247–62 (1967).

39. Vandamme, D., Courtillot, V., Besse, J. & Montigny, R. Paleomagnetism and age determinations of the Deccan Traps (India): Results of a Nagpur-Bombay traverse and review of earlier work. *Rev. Geophys.* **29**, 159–190, https://doi.org/10.1029/91RG00218 (1991).

40. Carlut, J. & Quidelleur, X. Absolute paleointensities recorded during the Bruhnes chron at La Guadeloupe Island. *Phys. Earth Planet. Inter.* **120**, 255–269 (2000).

41. De Groot, L. V., Biggin, A. J., Dekkers, M. J., Langereis, C. G. & Herrero-Bervera., E. Rapid regional perturbations to the recent global geomagnetic decay revealed by a new Hawaiian record. *Nat. Commun.* **4**, 2727, https://doi.org/10.1038/ncomms3727 (2013).

42. Glatzmaier, G. A., Coe, R. S., Hongre, L. & Roberts, P. H. The role of the Earth's mantle in controlling the frequency of geomagnetic reversals. *Nature.* **401**, 885–890 (1999).

43. Shcherbakova, V., Kovalenko, D., Shcherbakov, V. & Zhidkov, G. Paleointensity of the geomagnetic field in the Cretaceous (from Cretaceous rocks of Mongolia). *Izvestiya Phys. Solid Earth* **47**(9), 775–791 (2011).

44. Tauxe, L. & Staudigel, H. Strength of the geomagnetic field in the Cretaceous Normal Superchron: New data from submarine basaltic glass of the Troodos Ophiolite, *Geochem. Geophys. Geosyst.* **5**, Q02H06, https://doi.org/10.1029/2003GC000635 (2004).

45. Shcherbakova, V. V. *et al.* Was the Devonian geomagnetic field dipolar or multipolar? Palaeointensity studies of Devonian igneous rocks from the Minusa Basin (Siberia) and the Kola Peninsula dykes, Russia. *Geophys. J. Int.* **209**, 1265–1286 (2017).

46. Hawkins, L. M. A. *et al.* An exceptionally weak Devonian geomagnetic field recorded by the Viluy Traps, Siberia. *Earth Planet. Sci. Letts.* **506**, 134–145 (2019).

47. Kutzner, C. & Christensen, U. R. Simulated geomagnetic reversal sand preferred virtual geomagnetic pole paths. *Geophys. J. Int.* **157**, 1105–1118, https://doi.org/10.1111/j.1365-246X.2004.02309.x (2004).
48. Moulin, M. *et al.* Eruptive history of the Karoo lava flows and their impact on early Jurassic environmental change. *J. Geophys. Res. Solid Earth.* **122**, 738–772, https://doi.org/10.1002/2016JB013354 (2017).
49. Courtillot, V. E. & Renne, P. R. On the ages of flood basalt events. *C. R. Geosci.* **335**, 113–14 (2003).
50. Cottin, J. Y., MiChon, G. & DelpeCh, G. The Kerguelen volcanic Plateau: the second largest oceanic Igneous Province (LIP) on earth and a witness of the Indian Ocean opening. *The Kerguelen Plateau: marine ecosystem and fisheries: Societe Francaise d'lchtyologie* **35**, 29–42 (2011).
51. Gradstein, F., Ogg, J., Schmitz, M &, Ogg, G. The Geologic Time Scale 2012. Amsterdam, Elsevier Science. (2012).

Acknowledgements

Author contributions

R.T., designed the research, did data processing and wrote the manuscript; A.R.M. participated in sample collection, did the sample processing, working out experimental protocols and analysis; V.M. and S.G.S. associated in experimental work and data analysis; all authors edited the ms.

Competing interests

The authors declare no competing interests.

Additional information

Supplementary information is available for this paper at https://doi.org/10.1038/s41598-020-67245-6.

Correspondence and requests for materials should be addressed to R.T.

Reprints and permissions information is available at www.nature.com/reprints.

Publisher's note Springer Nature remains neutral with regard to jurisdictional claims in published maps and institutional affiliations.